Neutron Reflectivity Studies of End-Grafted Polymers

T. L. Mansfield,† D. R. Iyengar,‡ G. Beaucage,§ T. J. McCarthy, and R. S. Stein

Polymer Science and Engineering, University of Massachusetts, Amherst, Massachusetts 01002

R. J. Composto*

Materials Science and Engineering, University of Pennsylvania, Philadelphia, Pennsylvania 19104-6272

Received June 13, 1994; Revised Manuscript Received October 14, 1994®

ABSTRACT: Neutron reflectivity is used to measure the volume fraction profile of carboxylic acid-terminated polystyrene (PSCOOH) absorbed on silicon oxide from deuterated cyclohexane, a near-Θ solvent. Because of the affinity of the acid group for the silicon oxide surface, the PSCOOH adsorbed amount is 4 times larger than the unfunctionalized PS case at 23 °C. Although both PS and PSCOOH have similar surface volume fractions (ca. 0.60), the PSCOOH layer thickness is 4 times larger, suggesting that the PSCOOH chains stretch by 4 times their unperturbed size. Upon increasing the degree of polymerization N from 67 to 780, the PSCOOH layer thickness scales as N^1 under near-Θ solvent conditions. Under good solvent conditions, the PSCOOH surface volume fraction decreases by a factor of 3, whereas the layer thickness remains the same as in the near-Θ case. In both solvents, the reflectivity can be fit with PSCOOH profiles which are parabolic with some rounding near the free chain ends. Neutron reflectivity studies of DPSCOOH and PSCOOH adsorbed from cyclohexane and cyclohexane-d, respectively, suggest that DPSCOOH adsorption is slightly stronger due to isotope effects.

Introduction

End-adsorbed polymer chains, aside from their practical importance in the control of colloidal dispersions, are of great interest for testing the theoretical models which describe the structure of polymers attached by one end to a solid surface. Alexander[1] was the first to predict that densely packed tethered chains would stretch away from the surface such that their chain dimension normal to the wall is much larger than the unperturbed molecular size. When grafted to a surface and immersed in solvent, tethered chains stretch because of favorable solvent-segment interactions and/or excluded-volume interactions between neighboring chains. Thin layer chromatography experiments show that carboxylic acid-terminated polystyrene (PSCOOH) diffuses several orders of magnitude slower than unfunctionalized polystyrene, suggesting that the acid group interacts with the silica surface.[2] In this paper, PSCOOH is used as a model system to study the effect of terminal group species, molecular weight, solvent quality, and isotopic substitution on polymer adsorption.

In the first experiment, we will show that PS adsorption increases dramatically if a carboxylic acid group is attached to the chain end. In a previous publication[3] we demonstrated the feasibility of using neutron reflectivity to measure the volume fraction profile of PSCOOH in cyclohexane. Here, we extend these studies by determining the molecular weight dependence of the polymer concentration profile under near-Θ conditions. For all molecular weights, the profiles are found to be parabolic and have layer thicknesses which scale as the degree of polymerization to the first power. The effect of solvent quality is also presented. Whereas the PSCOOH thickness is the same in good (deuterated toluene) and near-Θ (deuterated cyclohexane) solvents, the surface volume fraction is 4 times larger in the near-Θ case. In the final study, the isotope dependence of polymer adsorption will be reexamined.[3]

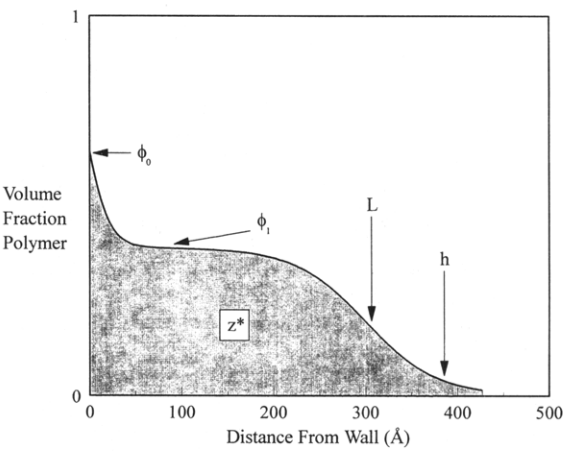

Figure 1. Sample polymer volume fraction profile and key parameters such as the surface concentrations, ϕ_0 and ϕ_1, the brush thickness and height, L and h, and surface excess, z^*.

Theory

Before describing theories which are relevant to our experimental conditions, the features which describe the polymer volume fraction profile are reviewed. As shown in Figure 1, the polymer volume fraction profile is defined by its shape $\phi(z)$, the volume fraction near the wall ϕ_1, and the layer thickness L. For end-grafted chains near an attracting surface, the surface volume fraction is expected to be greater than ϕ_1 and therefore another parameter, ϕ_0, is defined.[4−6] As shown later, this prediction is confirmed by experiments on the PSCOOH(81K) system. Although the profile shape has been of great interest for many years,[7] techniques with sufficient depth resolution, such as neutron reflectivity[3,8] and small-angle neutron scattering,[9] have only

† Present address: The Procter & Gamble Co., 6300 Center Hill Avenue, Cincinnati, OH 45224.

‡ Present address: Materials Science and Engineering, Cornell University, Ithaca, NY 14853.

§ Present address: Sandia National Laboratory, Albuquerque, NM 85051.

® Abstract published in *Advance ACS Abstracts,* December 15, 1994.

0024-9297/95/2228-0492$09.00/0

recently been applied to study polymer adsorption. In this paper, neutron reflectivity is used to measure the volume fraction profile.

From the volume fraction profile, the surface excess z^*, the distance between grafting sites d, the graft density σ, and the ellipsometric thickness L can be calculated. The surface excess is given by

$$z^* = \int_0^\infty dz\, (\phi(z) - \phi_\infty) \tag{1}$$

where ϕ_∞ is the bulk concentration of the polymer in solution. The surface excess is equivalent to the area under the $\phi(z)$ curve and represents the "collapsed" layer thickness of a dried film. The adsorbed amount, in units of polymer mass per unit area, is equal to the surface excess times the polymer density, ϱ_0. The average separation between attachment sites on the surface is

$$d = \left(\frac{NM_0}{z^*\varrho_0 N_a}\right)^{1/2} \tag{2}$$

where N_a, N, and M_0 represent Avogadro's number, the degree of polymerization, and the monomer molecular weight, respectively. The grafting density of chains attached to the wall is

$$\sigma = \frac{a^2}{d^2} = \frac{z^* a^2 \varrho_0 N_a}{NM_0} \tag{3}$$

where a is the monomer size. Chain stretching occurs at high values of σ, or when d is less than the unperturbed chain dimension $R_g = N^{0.5}a$. The layer thickness L is defined as the first moment of the profile

$$L = \frac{1}{z^*}\int_0^\infty dz\, z(\phi(z) - \phi_\infty) \tag{4}$$

For some systems, a brush height h can be defined if the polymer concentration decreases abruptly near the chain ends.[7] For similar profile shapes h scales with L. To avoid ambiguity the layer thickness in this paper means L unless otherwise stated.

Detailed reviews of polymer adsorption theory have been published elsewhere.[7,10,11] In this paper, we limit discussion to theories commensurate with our experimental conditions. These conditions correspond to the adsorption of moderate molecular weight (7K–81K) end-functionalized chains attached to a substrate at moderate to high grafting densities (0.02–0.062) under good and near-Θ conditions.[12] By balancing the interaction energy due to chain overlap with the elastic energy for chain stretching, Alexander[13] and de Gennes[14] (AdeG) predict an equilibrium thickness

$$L \sim (v\sigma)^{1/3}N \qquad \text{good solvent } (\chi < 0.5) \tag{5}$$

which scales with graft density, degree of polymerization, and the excluded-volume parameter v defined as $0.5 - \chi$, where χ is the Flory interaction parameter. Because of the strong stretching condition ($d \ll R_g$), the layer thickness scales linearly with N, in agreement with experimental results.[11] Although the AdeG model provides an accurate macroscopic description, this approach assumes a steplike polymer concentration profile and therefore ignores the molecular level details which control important properties such as the rheological behavior of colloids.

Using Flory arguments, Halperin[15] predicts that L varies as $N^{1.0}$ at high grafting densities. In Θ and poor solvents, this thickness varies as

$$L \sim \sigma^{1/2}N \qquad \text{theta solvent } (\chi = 0.5) \tag{6}$$

$$L \sim \sigma N|v|^{-1} \qquad \text{poor solvent } (\chi > 0.5) \tag{7}$$

The Halperin approach assumes a nonadsorbing surface and a free energy given by a third-order virial expansion. Note that eqs 5–7 predict that L varies as $N^{1.0}$, independent of solvent quality. For poor solvent conditions, Halpern predicts that L varies strongly with graft density because excluded-volume interactions become the main driving force for chain stretching as solvent quality decreases.

Self-consistent mean-field theories[16] are useful tools for calculating the volume fraction profiles of grafted polymers. For high molecular weight chains at moderately high coverage in a good solvent, Milner, Witten, and Cates (MWC)[17] use an analytic approach to solve for the volume fraction profile,

$$\phi(z) = A_0 - \beta_0 z^2 \qquad z \le h \tag{8}$$

where $A_0 \sim \sigma^{2/3}v^{-1/3}$ and $B_0 \sim v^{-1}N^{-2}$. The MWC approach predicts that $L \sim N$, in agreement with AdeG. Assuming large N and strong stretching conditions, Wijmans, Scheutjens, and Zhulina (WSZ)[18] extend the SCF theory of Zhulina, Priamitsyn, and Borisov[19] to high grafting densities and Θ and poor solvent conditions. In the WSZ theory, the volume fraction profile of grafted polymer in a Θ solvent is shaped like the square root of a parabola with rounding near the foot region due to fluctuation effects.

Numerical SCF calculations provide an alternative method for predicting the molecular weight, grafting density, and solvent quality dependence of polymer adsorption. Because the numerical SCF theory relaxes the strong stretching condition, the theory is applicable to a wider variety of experimental conditions than the analytical SCF theory. Cosgrove et al.[20] and Hirz[21] first applied the numerical SCF theory to polymer brushes. As a novel feature, Cosgrove includes an attractive interaction between the surface and the chain segments by defining an interaction parameter χ_a. Upon increasing χ_a from 0 to 0.5 (i.e., from a noninteracting to an attractive surface), the volume fraction profile shape changes from nearly parabolic to exponential as chain segments become increasingly attracted to the surface. Recently, Whitmore and Noolandi[22] (WN) used a numerical SCF approach to calculate the volume fraction profile as a function of solvent quality, surface coverage, and degree of polymerization. WN report layer thicknesses given by

$$L \sim \sigma^{1/4}N^{4/5} \qquad \Theta \text{ solvent } (\chi = 0.5) \tag{9}$$

$$L \sim \sigma^{2/5}N^{3/5} \qquad \text{poor solvent } (\chi = 0.6) \tag{10}$$

$$L \sim \sigma^{0.3}N^{>4/5} \qquad \text{good solvent } (\chi = 0.4) \tag{11}$$

For all solvent conditions, L scales more weakly with N and σ than in the Flory predictions shown in eqs 5–7. This difference may be due to the low grafting density range ($0.02 > \sigma > 0.001$) studied by WN. WN also provide scaling predictions for the surface volume fraction

$$\phi_1 \sim \sigma^{1/2}N^{1/12} \qquad \text{theta solvent} \qquad (12)$$

$$\phi_1 \sim \sigma^{1/4}N^{1/8} \qquad \text{poor solvent} \qquad (13)$$

As solvent quality decreases or N increases, the free energy penalty for chain overlap decreases and therefore the polymer segment density near the wall increases. As discussed later, the surface volume fraction in a near-Θ solvent can be 3 times larger than that in a good solvent.

The theories reviewed in this section apply to polymer chains that are grafted at one end onto a solid surface. As in many problems, the theoretical framework does not exactly match the experimental one. In particular, attached PSCOOH chains are not irreversibly bound to the oxide surface. Thus the coverage or graft density of PSCOOH will be determined by balancing the COOH/solid interaction against the osmotic pressure which stretches the chain. Hence, the coverage is expected to depend on the strength of the COOH/SiO_2 interaction which is 1.6×10^4 J/mol or 6.4 kT.[23] As shown below, this prediction is consistent with measurements of the layer thicknesses in good and near-solvents.

Experimental Section

Materials. Adsorption studies of deuterated polystyrene (DPS), carboxylic acid-terminated polystyrene (PSCOOH), and carboxylic acid-terminated deuterated polystyrene (DPSCOOH) are reported in this paper. The polymer synthesis procedure was published elsewhere.[24] In all cases, polymerizations were initiated with *sec*-butyllithium, and therefore the polymers were terminated on one end with a secondary butyl group end. The other chain end was capped with either a carboxylic acid group or a proton, depending on the termination reaction. For the functionalized polystyrenes, the end-capping yields were 90% or greater.[2] The number-average degrees of polymerization, polydispersity indexes, and code names of the polymers are shown in Table 1. The code names were derived from the hydrogen isotope (first letter), the weight-average molecular weight ($\times 10^3$), and the chemical group on the chain terminus, C for a COOH and H for proton.

Procedure. The NR measurements were performed on the BT-7 reflectometer at the National Institute of Standards and Technology. A graphite monochromator was used to select neutrons of wavelength $\lambda = 2.367$ Å with $\Delta\lambda/\lambda = 0.01$. The horizontal angular resolution of the incoming beam was varied from 0.015° to 0.03° during the specular scans.[25] The reflectivity was measured as a function of the scattering wave vector, $k = 2\pi/\lambda \sin\theta$, where θ is the incident angle between the sample and incident beam. The neutron reflectivity technique and data analysis procedures have been discussed in detail elsewhere.[26]

The polymer volume fraction profile normal to the solid/solution interface was determined using neutron reflectivity. To contrast the polymer from its environment, PSCOOH was dissolved in deuterated cyclohexane (a near-Θ solvent) or deuterated toluene (a good solvent). Similarly, DPS and DPSCOOH were dissolved in cyclohexane. A polymer concentration of 1.5 mg/cm^3 was chosen to ensure dilute solution conditions. With respect to the overlap concentration c^*, this polymer concentration corresponds to $c^*/100$. The solid surface was a single-crystal silicon brick (20 × 10 × 2.5 cm) which was seated in a quartz cell end-capped with polished windows (0.5 mm thick). The incident neutron beam entered the cell window, passed through the silicon, reflected off the silicon–solution interface, and again traversed the silicon before passing through the other window. To produce a well-defined surface, the silicon (and cell) was washed in a toluene bath, cleaned with a H_2SO_4–$KClO_3$ solution, rinsed with distilled water, and dried in a nitrogen atmosphere. The polymer solution was injected into a ~2 mm gap between the silicon and cell face and allowed to equilibrate for at least 2 h before initiating data collection. In most cases, a reflectivity spectrum was measured in 12 h. In selected experiments, the reflectivity was measured a second time, immediately after the first run. To within experimental error, the reflectivity was stable for several days, in agreement with previously reported experiments.[27] In the highest molecular weight case (H81C), the reflectivity showed a slight time dependence at high k, suggesting that equilibrium was not yet achieved. To check reproducibility, the reflectivity from D14C was measured on two separate occasions, about 6 months apart. Within experimental error, both measurements were in excellent agreement.

Table 1. Polymer Characteristics and Code Names

polymer	degree of polymzn	polydispersity index	code name
DPS	125	1.06	D14H
DPSCOOH	122	1.04	D14C
PSCOOH	67	1.10	H7C
PSCOOH	114	1.04	H12C
PSCOOH	220	1.07	H23C
PSCOOH	788	1.09	H81C

Analysis of Reflectivity Data. The volume fraction profile was determined by comparing the experimental reflectivity with the theoretical reflectivity calculated from a model scattering length density profile $\varrho(z)$. In the $\varrho(z)$ model, the roughnesses at the Si–SiO_2 and SiO_2–solution interfaces were represented by convoluting $\varrho(z)$ with a Gaussian function having a fwhm of 10.8 Å. The reflectivity from the model profile was calculated using the matrix method based on the Fresnel theory of reflectivity. The features of the profile were adjusted using a Levenburg–Marquardt nonlinear least-squares algorithm.[28] The χ^2 fits were improved by including a layer of water (ca. 4 Å) at the solution–SiO_2 interface.[29]

After determining $\varrho(z)$ from reflectivity measurements, the polymer volume fraction profile $\phi(z)$ was calculated,

$$\phi(z) = (\varrho(z) - \varrho_s)/(\varrho_p - \varrho_s) \qquad (14)$$

where ϱ_s and ϱ_p are the solution and polymer scattering length densities, respectively. The model profiles were calculated from

$$\phi(z) = \phi_\infty + \left[\frac{1-\phi_\infty}{1-\tanh(z_c/\lambda)}\right]\left[1 - \tanh\left(\frac{z}{\lambda}\right) - z_c\right] \qquad (15)$$

where λ is the characteristic thickness of the adsorbed layer. By varying z_c, this profile can represent an error function ($z_c = 0$), parabolic ($z_c > 0$), or exponential ($z_c < 0$) profile. The reflectivity was also simulated using a parabolic profile

$$\phi(z) = \phi_\infty + (\phi_1 - \phi_\infty)(1 - z^2/h^2) \qquad z \le h \qquad (16)$$

Near $z = h$, this parabolic profile was "rounded" by convoluting eq 16 with a Gaussian function having a continuously-varying width which has a maximum value of ~15 Å. Under near-Θ conditions and at high grafting densities, SCF theory predicts that the square of the profile is parabolic with rounding near the foot.[18] Because of their similar shape, this profile and a rounded parabola are indistinguishable in our NR simulations. For consistency, a rounded parabola profile will be used to analyze the data in this paper. As discussed in the Results and Discussion section, reflectivity simulations based on eq 15 or eq 16 are in excellent agreement with the experimental reflectivities. In the case of H81C, the profiles were modified by adding an exponentially decaying polymer excess near $z = 0$ (see Figure 1). The driving force for this excess is an attractive interaction between the polymer segments and the adsorbing surface.[4,6]

Before presenting experimental results, the sensitivity of NR to the various regions of the scattering length density profile should be addressed. In general, NR is most sensitive to sharp $\varrho(z)$ gradients, such as at the solution–silicon ($z = 0$) or chain end–solution ($z = L$) interfaces. However, NR is less

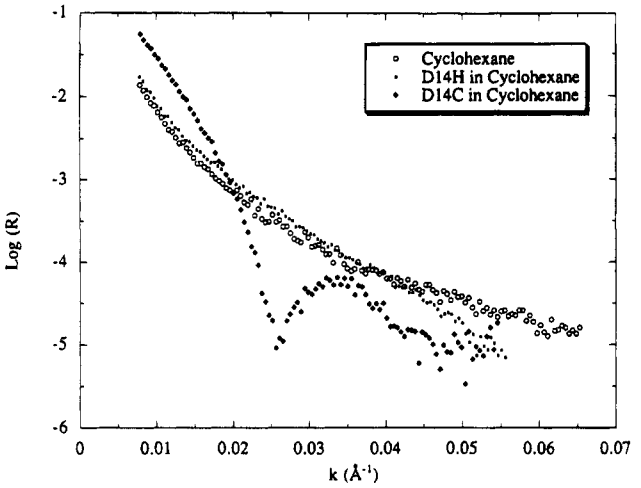

Figure 2. Neutron reflectivity spectra of D14H, D14C, and cyclohexane at 23 °C.

sensitive to gradual $\varrho(z)$ gradients, for example, at intermediate z values. Therefore, NR is very sensitive to ϕ_1, L, and the shape of the profile (i.e., concave vs convex) but is less sensitive to distinguishing between profiles with similar shapes (i.e., error function vs parabolic). A detailed discussion of the advantages and disadvantages of neutron reflectivity has been given elsewhere.[26]

Results and Discussion

Terminal Group Dependence. At high grafting densities, terminally attached chains stretch away from the interface, producing a layer thickness which is much greater than R_g, the unperturbed chain dimension. To provide evidence of chain stretching, the reflectivities of D14H and D14C in cyclohexane are compared in Figure 2. Whereas the reflectivity from D14H (squares) is featureless, the reflectivity from D14C (diamonds) displays a sharp interference minimum near $k \approx 0.026$ Å^{-1}, indicating that neutrons reflected from the front ($z = 0$) and back ($z = L$) of the adsorbed layer interfere with each other. Such interference can only occur if the polymer volume fraction profile is convex, for example, parabolic; a concave profile (e.g., exponential) decays too gradually to produce interference minima. Thus, reflectivity fringes provide a qualitative indication of the profile shape.

Figure 2 also shows that the reflectivity from pure cyclohexane (circles) is featureless. A simulation to this data provides the oxide thickness, oxide roughness, and cyclohexane scattering length density, which are 15 Å, 11 Å, and -1.0×10^{-6} Å^{-2}, respectively. These values are used in all subsequent simulations. Figures 3 and 4 show the reflectivity spectra for D14C and D14H, respectively. For both polymers, the agreement between experiment and simulation is excellent. The insets show the scattering length density profiles used in the simulations. Starting at $z = 0$, these scattering length profiles represent the silicon substrate, a silicon oxide layer, a monolayer of water, the adsorbed polymer layer, and the solution.

Figure 5 shows the polymer volume fraction profiles calculated from the scattering length density profiles shown in Figures 3 and 4. The D14H profile is parabolic with a rounding of 16 Å fwhm at $z = L$. As predicted by numerical SCF calculations,[21,22,30] a parabolic profile also provides a good description of D14C adsorption. From the polymer volume fraction profile, the adsorbed amount, layer thickness, and distance between grafting sites are determined. Figure 5 shows that the functionalization of PS produces a dramatic 4-fold increase in the adsorbed amount. This increase in z^* is mainly attributed to an increase in the layer thickness from 24 Å, ca. R_g (=32 Å), to 105 Å, ca. $3R_g$. After rinsing

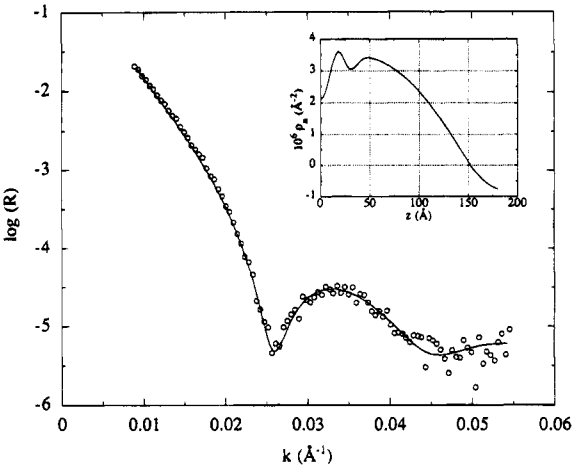

Figure 3. Experimental (symbols) and calculated (solid line) reflectivity for D14C in cyclohexane. The solid line was calculated using the scattering length density profile shown in the inset. The silicon oxide and water monolayer produce the ϱ_n features at $z \approx 10$ and 20 Å, respectively.

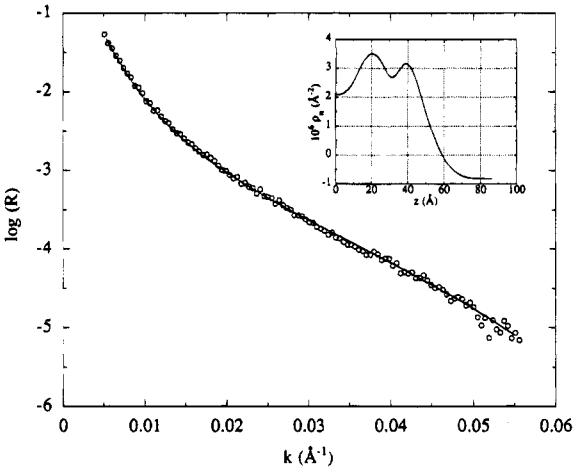

Figure 4. Experimental (symbols) and calculated (solid line) reflectivity for D14H in cyclohexane. The solid line was calculated using the scattering length density profile shown in the inset. The oxide and water monolayer produce the ϱ_n features at $z \approx 20$ and 30 Å, respectively.

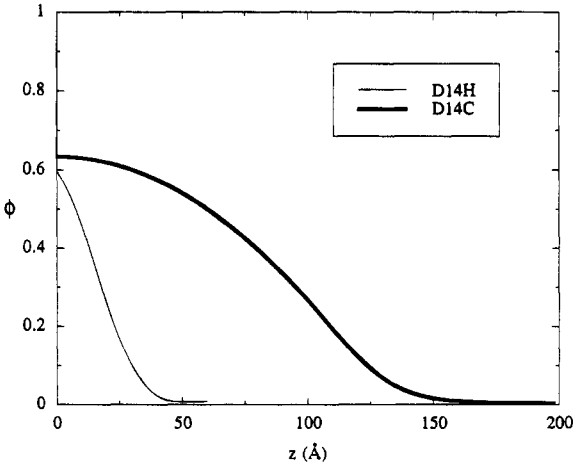

Figure 5. Volume fraction profiles of D14H and D14C in cyclohexane. These profiles were calculated from the ϱ_n shown in Figures 3 and 4.

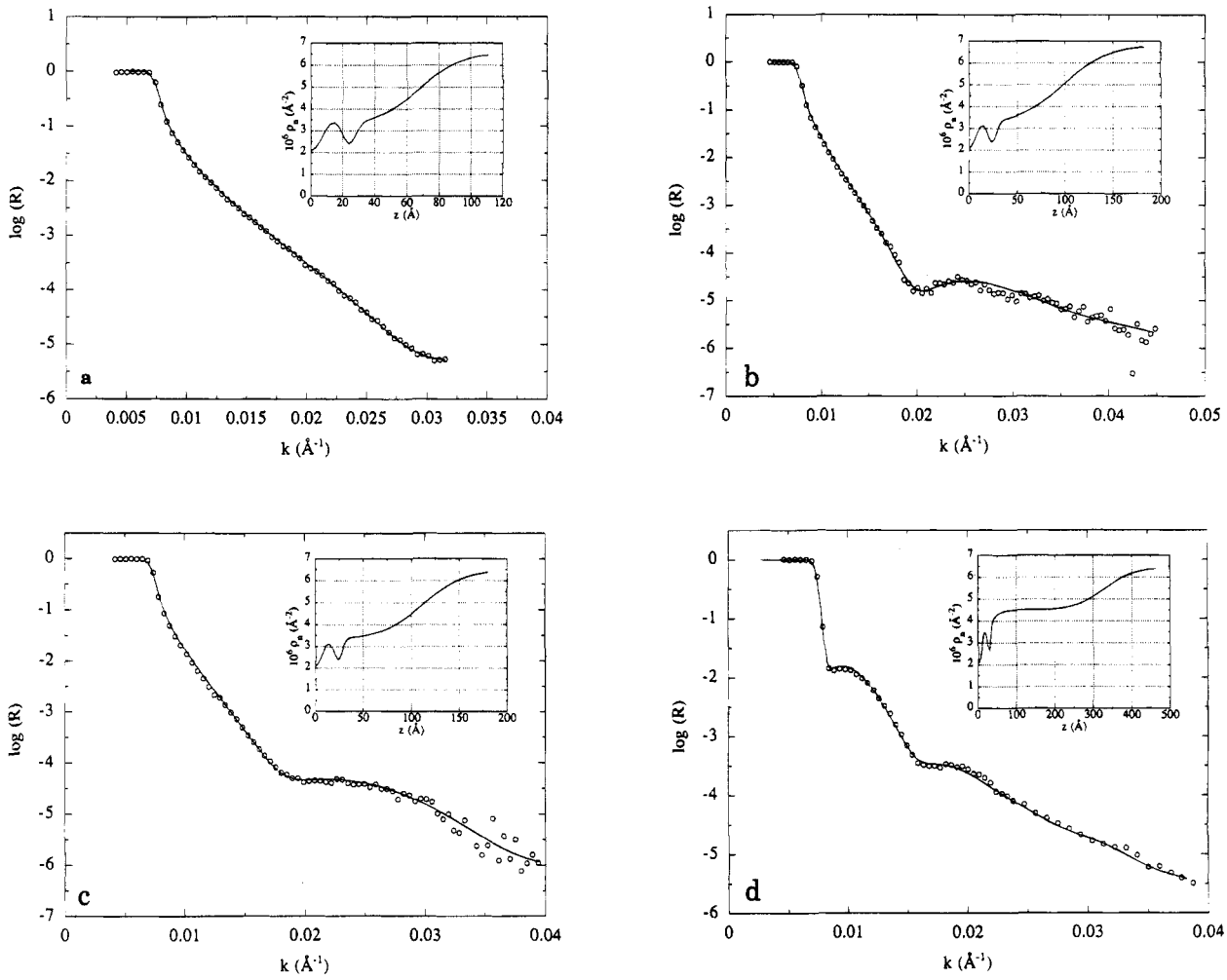

Figure 6. Comparison of calculated (solid line) and observed NR for (a) H7C, (b) H12C, (c) H23C, and (d) H81C in cyclohexane-*d*. The solid lines were calculated from the scattering length densities shown in the insets.

and drying the adsorbed D14C layer, the z^* measured by forward-recoil spectrometry and X-ray reflectivity were within 5% of the in situ NR value. This result suggests that the D14C layer is monomolecular and strongly attached to the substrate.[31] The average distance between COOH attachment sites is 20 Å. Given that $d < R_g < L$, D14C adsorption from cyclohexane falls under the category of a moderately stretched polymer brush.[11] In contrast, the unfunctionalized D14H chains have an effective d of 41 Å, which suggests that these chains are unperturbed.

Whereas the adsorbed amount of D14C is 4 times greater than that of D14H, the surface concentrations ϕ_1 of the carboxylic acid- and hydrogen-terminated polystyrenes are both ca. 0.60. This observation indicates that the styrene–oxide interaction determines ϕ_1 for adsorption under near-Θ conditions. Using neutron reflectivity, Cosgrove et al.[32] measured the adsorption of DPS ($N \sim 500$) from cyclohexane onto mica, finding that ϕ_1 is ca. 0.15. Because of the weak adsorption of DPS and the limited k range studied, these reflectivity measurements were insensitive to the details of the profile shape. As discussed below, we observe surface volume fraction values near 0.60, independent of PSCOOH molecular weight.

Molecular Weight Dependence. The molecular weight dependence of the polymer volume fraction profile was measured for the adsorption of PSCOOH in cyclohexane-*d* at 23 °C, a temperature 17 °C below the Θ temperature of PS/cyclohexane-*d*.[33] Parts a–d of Figure 6 show the reflectivities (symbols) from PSCOOH having degrees of polymerization 67, 114, 220, and 788, respectively. The insets show the scattering length density profiles used to calculate the simulated reflectivities (solid lines). The angles at which total external reflection ($R = 1$) occurs are determined by the scattering length of the bulk solution; therefore, the critical values of k are similar in parts a–d of Figure 6. As N increases, the period of the interference oscillations is observed to decrease. At low N (H7C), this period is outside the k range. For intermediate N (H12C and H23C), a reflectivity minimum is observed near $k = 0.02$ Å^{-1}. For the highest N (H81C), two minima are clearly observed. Qualitatively, this decrease in the reflectivity period Δk can be attributed to an increase in the adsorbed layer thickness, $\Delta k \sim \pi/L$.

Figure 7 shows the polymer volume fraction profiles calculated from the scattering length profiles shown in the insets of parts a–d of Figure 6. For all N's, the shape of the volume fraction profile is parabolic with some rounding near $z = L$. For the highest N, the profile shows a polymer excess near $z = 0$. This excess has been predicted for end-grafted chains attached to a surface which has a short-range attraction for the chain segments.[4,6] Given that PS does indeed absorb from cyclohexane (see Figure 5), the observation of a polymer excess near the wall is reasonable. For the three lowest N's, the reflectivity can be fit without including a polymer excess near $z = 0$. This behavior may be explained by considering the effect of N on the solvent

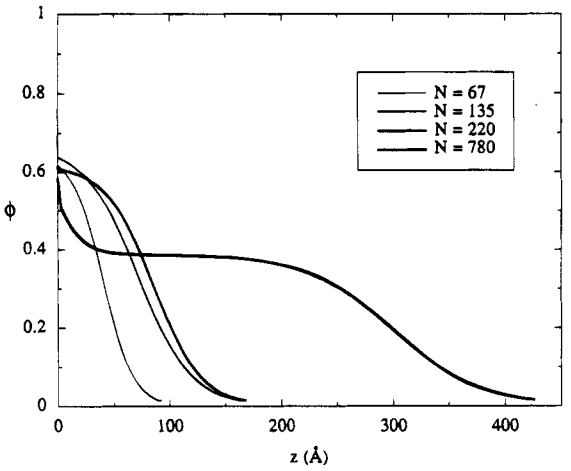

Figure 7. Volume fraction profiles of H7C, H12C, H23C, and H81C in cyclohexane-*d*. These profiles were calculated from the ϱ_n shown in parts a–d of Figure 6.

Table 2. PSCOOH Adsorbed Layer Characteristics Obtained from Reflectivity Simulations

polymer	L (Å)[a]	ϕ_1[a]	z^* (Å)[a]	d (Å)[a]	σ[a]
H7C	51 ± 1	0.62 ± 0.02	27 ± 3	20 ± 2	0.062 ± 0.005
H12C	92 ± 1	0.64 ± 0.01	49 ± 3	21 ± 1	0.056 ± 0.005
H23C	100 ± 1	0.61 ± 0.01	54 ± 3	26 ± 2	0.037 ± 0.004
H81C	306 ± 4	0.39 ± 0.01	121 ± 5	33 ± 4	0.023 ± 0.002

[a] 95.4% confidence limit.[28]

quality, $\chi_s - \chi$, where χ_s is the spinodal χ value. Because an increase in N will decrease $\chi_s - \chi$, the segment–solvent interactions become less favorable. This effect can enhance the segment adsorption on the substrate. Also, at low N, NR may be insensitive to small values of the polymer excess near $Z = 0$. Note that the surface concentration is ca. 60% for all N. However, the layer thickness increases with increasing N. The fitting parameters (L and ϕ_1), surface excess, distance between grafting sites, and grafting density are given in Table 2. The layer thickness of this N series is described by

$$L \sim \sigma^{0.73} N^{1.0} \tag{17}$$

Because eq 17 is based on only four values of N, the scaling exponents are only approximate values. Nevertheless, the σ scaling exponent of 0.73 falls between the predicted values for Θ and poor solvents, which are 0.5 and 1.0, respectively.[15] This result seems reasonable for the PS/cyclohexane-*d* system at 23 °C, where χ = 0.53.[33] Furthermore, at high grafting densities, Halperin predicts that L varies as $N^{1.0}$ for Θ and poor solvent conditions, in excellent agreement with eq 17. Note that Whitmore and Noolandi predict (eqs 9 and 10) that L depends more weakly on σ and N than the scaling behavior shown in eq 17. This discrepancy may result from the low grafting density range explored by WN compared with the σ's shown in Table 2.

Solvent Quality Dependence. The equilibrium shape of a polymer brush is determined by balancing the free energy costs for chain stretching and chain overlap. Chains stretch away from an interface so as to maximize solvent–segment interactions (good solvent conditions) and/or to avoid overlap with neighboring chains (excluded volume). To understand the role of solvent quality, reflectivity was measured for H12C in cyclohexane-*d* and toluene-*d* at 23 °C. These solvents correspond to near-Θ and good solvent conditions,

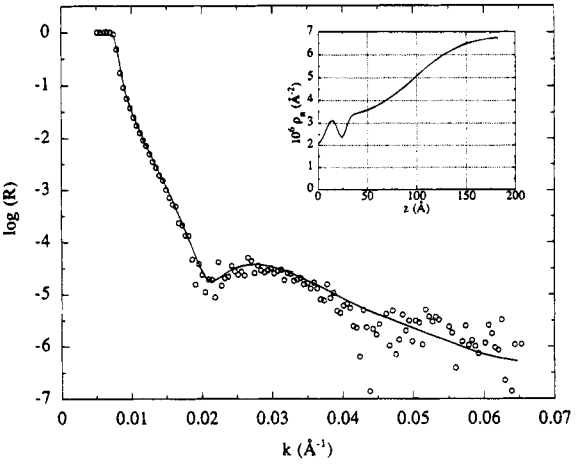

Figure 8. Experimental (symbols) and calculated (solid line) reflectivity for H12C in cyclohexane-*d* at 23 °C. The solid line was calculated using the ϱ_n shown in the inset.

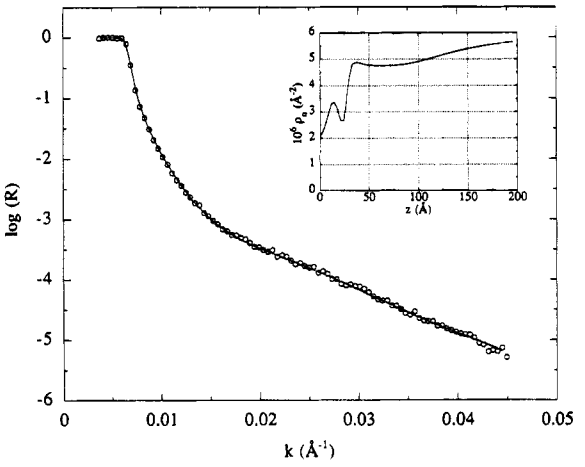

Figure 9. Experimental (symbols) and calculated (solid line) reflectivity for H12C in toluene-*d*, a good solvent. The solid line was calculated using the ϱ_n shown in the inset.

respectively. Figure 8 shows that the reflectivity from cyclohexane-*d* displays an interference minimum, suggesting that the volume fraction profile is relatively sharp near the chain ends. In contrast, Figure 9 shows that the reflectivity from toluene-*d* monotonically decreases. Good fits (solid lines) to the reflectivity are obtained from the scattering length density profiles shown in the insets of Figures 8 and 9. Note that Figures 6b and 8 represent independent H12C adsorption measurements separated in time by 6 months. Within experimental error the scattering length density profiles are identical.

Figure 10 shows the volume fraction profiles of H12C calculated from the insets in Figures 8 and 9. For both cyclohexane-*d* and toluene-*d*, the profiles are parabolic with rounding near $z = L$. Recall that our NR measurements cannot distinguish between this profile and one shaped like the square root of a parabola with rounding. Interestingly, the absorbed layer thicknesses are ca. 100 Å, independent of solvent quality. Whereas excluded-volume dictates chain stretching in cyclohexane-*d*, both excluded-volume and favorable solvent–segment interactions stimulate chain extension in toluene, a good solvent having $\chi = 0.43$.[12] Therefore, the similar layer thicknesses found in cyclohexane-*d* and toluene-*d* suggest that chain stretching is ultimately determined by the interaction between carboxylic acid and silicon oxide.[2] In contrast, the surface volume fraction is very

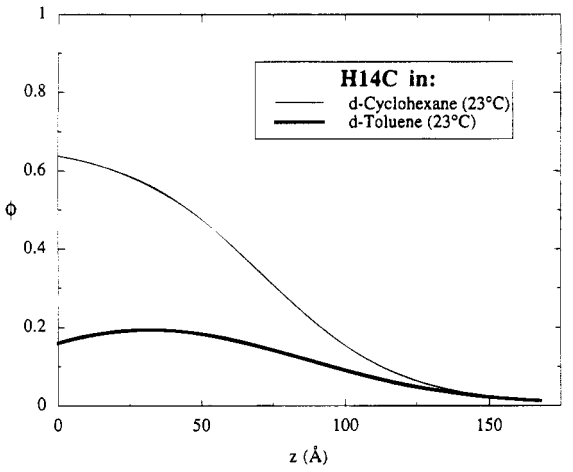

Figure 10. Volume fraction profiles of H12C in toluene-*d* and cyclohexane-*d*, good and near-Θ solvents, respectively. These profiles were calculated from the ϱ_n's shown in Figures 8 and 9.

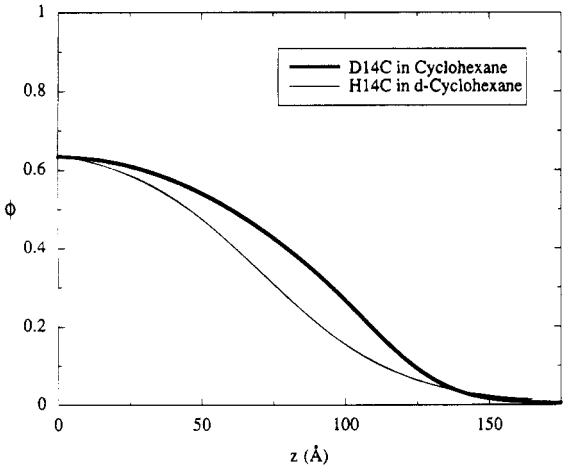

Figure 11. Volume fraction profiles of H12C and D14C in cyclohexane-*d*, and cyclohexane at 23 °C. The degrees of polymerization for H12C and D14C and 114 and 122, respectively. The reflectivity data were published in ref 3.

sensitive to solvent quality. Figure 10 shows that a decrease in solvent quality will increase the surface volume fraction in qualitative agreement with SCF predictions, eqs 12 and 13. Moreover, a small depletion layer is observed for PSCOOH adsorption from toluene-*d* but not in the cyclohexane-*d* case, suggesting that χ_a is relatively weaker for the PSCOOH/toluene-*d* system.

Isotope Dependence. Because isotopic mixtures are often used to contrast match the bulk solution and substrate, the effect of isotopic substitution on the adsorption of end-functionalized polymers is of interest. Figure 11 shows the polymer volume fraction profiles of H12C and its isotopic complement D14C in cyclohexane-*d* and cyclohexane, respectively. The layer thickness and coverage of D14C are both about 15% greater than that in the H12C case. This result can be partly explained by the difference in the degrees of polymerization, 122 and 114, between D14C and H12C, respectively. Deuterated polystyrene in cyclohexane has been found to adsorb more strongly than polystyrene from the same solvent.[34] Although the isotope effect in our system is not very strong, the larger adsorption of end-functionalized deuterated polystyrene is in qualitative agreement with the homopolymer results in ref 34.[35]

Conclusions

Neutron reflectivity has been used to obtain the volume fraction profiles of DPS and DPSCOOH in cyclohexane, a near-Θ solvent. For both DPS and DPSCOOH, the polymer volume fraction is parabolic with rounding near the free chain ends; however, the DPSCOOH chains are extended by ca. $4R_g$, whereas the DPS chains are ca. R_g. Under near-Θ conditions, the PSCOOH layer thickness scales as $N^{1.0}$ and $\sigma^{0.7}$, in agreement with Halperin's predictions. Upon adsorbing PSCOOH from toluene, a good solvent, the layer thickness is the same as that in the near-Θ case; however, the surface concentration decreases by ca. 3 times. This result suggests that the carboxylic acid–silicon oxide interaction is the dominant factor which determines layer thickness. The adsorption measurements of DPSCOOH and PSCOOH from cyclohexane and cyclohexane-*d*, respectively, suggest that isotopic labeling has a small effect on adsorption.

Acknowledgment. We thank Drs. T. P. Russell, F. Bates, and S. Patel for their comments. The research was supported by NSF Grants DMR 91-58462 (R.J.C.) and DMR-8718420 (T.J.M.) and the NSF/Material Research Laboratories at UP (R.J.C.) and UMASS (T.J.C. and R.S.S.). Acknowledgment is made to the donors of the Petroleum Research Fund, administered by the ACS, for partial support of this research (R.J.C.). The support of Monsanto Chemical Co. (T.L.M., R.S.S., and R.J.C.) is gratefully acknowledged.

References and Notes

(1) Alexander, S. *J. Phys. Fr.* **1977**, *38*, 977.
(2) Iyengar, D. R.; McCarthy, T. J. *Macromolecules* **1990**, *23*, 4344.
(3) Composto, R. J.; Mansfield, T.; Beaucage, G.; Stein, R. S.; Iyengar, D. R.; McCarthy, T. J.; Satija, S. K.; Ankner, J. F.; Majkrak, C. R. F. *MRS Symposium Proceedings*; Sirota, E. B., Weitz, D., Witten, T., Israelachvili, J., Eds.; Materials Research Society: Pittsburgh, PA, 1992; Vol. 248, pp 407–412.
(4) Chakrabarti, A.; Nelson, P. R. *Phys. Rev. A* **1992**, *49*, 4930.
(5) Cosgrove, P. *J. Chem. Soc., Faraday Trans.* **1990**, *86*, (9), 1323–1332.
(6) Marko, J. F.; Johner, A.; Marques, C. *J. Chem. Phys.* **1993**, *99*, N10, 8142.
(7) Milner, S. T. *Science* **1991**, *251*, 905.
(8) Satija, S. K.; Majkrzak, C. F.; Russell, T. P.; Sinha, S. A.; Sirota, E. B.; Hughes, G. J. *Macromolecules* **1990**, *23*, 3860–3864.
(9) Auroy, P.; Mir, Y.; Auvray, L. *Phys. Rev.* **1992**, *69*, 93.
(10) Kawaguchi, M.; Takahash A. *Adv. Colloid Interface Sci.* **1993**, *37*, 219.
(11) Halperin, A.; Tirrell, M.; Lodge, T. P. *Adv. Polym. Sci.* **1992**, *100*, 31.
(12) *CRC Handbook of Polymer–Liquid Interactions*; Barton, A. F. M., Ed.; CRC Press: Boca Raton, FL, 1990.
(13) Alexander, S. *J. Phys. (Paris)* **1977**, *389*, 83.
(14) de Gennes, P.-G. *J. Phys. (Paris)* **1976**, *37*, 1445; *Macromolecules* **1980**, *13*, 1069.
(15) Halperin, A. *J. Phys. (Paris)* **1988**, *49*, 547.
(16) Dolan, A. K.; Edwards, S. F. *Proc. R. Soc. London* **1975**, *A343*, 427.
(17) Milner, S. T.; Witten, T. A.; Cates, M. E. *Europhys. Lett.* **1988**, *5* (5), 413; *Macromolecules* **1988**, *21*, 2610.
(18) Wijmans, C. M.; Scheutjens, J. M. H. M.; Zhulina, E. B. *Macromolecules* **1992**, *26*, 2657.
(19) Zhulina, E. B.; Priamitsyn, V. A.; Borisov, O. V. *Polym. Sci. USSR* **1989**, *31*, 205.
(20) Cosgrove, T.; Heath, T.; van Lent, B.; Leeermakers, F.; Scheutjens, J. *Macromolecules* **1987**, *20*, 1692.
(21) Hirz, S. J. M.S. Thesis, The University of Minnesota, Minneapolis, MN, 1986.
(22) Whitmore, M. D.; Noolandi, J. *Macromolecules* **1990**, *23*, 3321.
(23) Frantz, P.; Leonhardt, D. C.; Granick, S. *Macromolecules* **1991**, *24*, 1868.
(24) Quirk, R. P. *Macromolecules* **1989**, *22*, 85.

(25) Majkrzak, C. F.; Satija, S. K. Private communication.
(26) Russell, T. P. *Mater. Sci. Rep.* **1990**, *5* (4,5), 171–271 and references therein.
(27) Motschmann, H.; Stamm, M.; Toprakcioglu, Ch. *Macromolecules* **1991**, *24*, 3681.
(28) Press, W. H.; Flannery, B. P.; Teukolsky, S. A.; Vetterling, W. J. *Numerical Recipes*; Cambridge University Press: Cambridge, U.K., 1986.
(29) Field, J. B.; Toprakcioglu, C.; Ball, R. C.; Stanley, H. B.; Dai, L.; Barford, W.; Penfold, J.; Smith, G.; Hamilton, W. *Macromolecules* **1992**, *25*, 434.
(30) Shull, K. Unpublished results.
(31) Perahia, D.; Wiesler, D. B.; Satija, S. K.; Fetters, L. J.; Sinha, S. K.; Milner, S. T. *Phys. Rev. Lett.* **1994**, *72*, 100–103.
(32) Cosgrove, T.; Heath, T. G.; Phipps, J. S.; Richardson, R. M. *Macromolecules* **1991**, *24*, 94–98.
(33) Strazielle, C.; Benoit, H. *Macromolecules* **1975**, *8*, 203.
(34) Leonhardt, D. C.; Johnson, H. E.; Granick, S. *Macromolecules* **1990**, *23*, 687.
(35) Note that the system in ref 34 is PS in cyclohexane.

MA9410882